Emulating one-dimensional resonant Q-matching behavior in a two-dimensional system via Fano resonances

David L. C. Chan,[1] Ivan Celanovic,[2] J. D. Joannopoulos,[1] and Marin Soljačić[1]
[1]*Department of Physics and Center for Materials Science and Engineering, Massachusetts Institute of Technology, Cambridge, Massachusetts 02139, USA*
[2]*Laboratory for Electromagnetic and Electronic Systems, Massachusetts Institute of Technology, Cambridge, Massachusetts 02139, USA*
(Received 16 May 2006; published 22 December 2006)

Through detailed numerical and analytical studies, we establish that the significant enhancement of thermal emission via Q matching, which has been possible in one-dimensional (1D) systems only, can be extended to two-dimensional (2D) systems by means of Fano resonances in the 2D system. In particular, we show the existence of essentially 1D behavior in a 2D system—a case of reduced dimensionality. Moreover, we show how properties of these spectra can be controlled by changing the geometrical parameters of the 2D system.

DOI: 10.1103/PhysRevA.74.064901 PACS number(s): 42.70.Qs

It has been noted recently that periodic subwavelength scale patterning of metallodielectric systems, i.e., photonic crystals, can modify their thermal-emission spectra in anomalous and intriguing ways [1–9]. As far as one-dimensional (1D) periodic photonic crystals go, one can control the thermal-emission spectra [10,11], generate coherent thermal emission [12,13], and also enhance thermal emission via resonant cavities [14]. Thermal radiation from two-dimensional (2D)-periodic photonic crystals has been studied within the contexts of spectral and directional control [3,16,17], guided resonances [18], thermophotovoltaic generation [7], and Kirchhoff's law [8]. And most recently, Laroche *et al.* [19] predicted coherent thermal emission due to leaky surface waves in truncated photonic crystal structures.

The body of work on enhancement of thermal emission via resonant cavities will interest us the most. One-dimensional systems are reducible to the problem of having one input channel, a resonant cavity, and one output channel, which provides excellent control over the transmission, reflection and absorption properties of such systems. In particular, by matching the radiative Q factor of a system with its absorptive Q factor, as in Ref. [14], one can greatly enhance thermal emission at the resonant frequency. In such a setup, light emitted by the resonant cavity and the incident light interfere so as to extremize the net outgoing wave. This complete cancellation of waves from the cavity and the incident or outgoing beam is unique to 1D systems. Thus, enhancement via Q matching, or critical coupling [15] an essentially 1D phenomenon, would not be expected to work in a general 2D system with multiple input or output channels.

In this Brief Report, we show that enhancement of thermal emission via Q matching, which is usually observed in 1D systems only, can be extended to 2D systems by coupling into Fano resonances [18] (arising from bulk guided modes of an otherwise uniform slab) in the 2D system. This mechanism differs from all those described above. In particular, we show the existence of essentially 1D behavior in a 2D system—a case of reduced dimensionality. (Note that 1D resonant scattering behavior can often be observed whenever modes are mapped to the Γ point.) In Fig. 1, we show how this can lead to anomalous behavior in thermal emission. We demonstrate through detailed numerical and analytical studies that the Fano resonances characteristic of 2D-periodic photonic crystal slabs can be understood in terms of a 1D model based on Q matching. We also show how properties of these thermal-emission spectra can be altered by changing the geometrical parameters of the system. Our mechanism differs from that by Greffet *et al.* [12] in that we consider coupling to the *bulk guided modes* in a *2D-periodic* system whereas in Ref. [12] the authors' work is based on coupling to *surface-phonon polaritons* in a *1D-periodic* system. But our work is different in a broader, more conceptual sense: we claim that by coupling to certain modes of a 2D periodic system, that system can be made to emulate 1D resonant scattering, and this behavior allows one to take advantage of Q matching, which is a fundamentally one-dimensional phenomenon. It turns out that this argument can also be applied to the system studied by Greffet *et al.*

A photonic crystal (PhC) slab with a 2D-periodic array of holes gives rise to a number of Fano resonances [18], as shown in Fig. 2(a). The way to understand these resonances is to note that radiation incident from the surrounding low-ϵ medium cannot couple into the guided modes of a uniform high-ϵ slab with continuous in-plane translational symmetry because of the conservation of the in-plane (transverse) wave vector. However, when the slab is punctuated with a periodic array of holes, dips, or other such perturbations, the transverse wave vector is conserved only up to a reciprocal lattice vector, and coupling between the incident radiation and the guided modes of the slab is now possible. The interaction between the guided modes and the incident radiation manifests itself in the form of very sharp peaks in the transmission spectrum [shown in Fig. 2(a)], called Fano resonances. Fano resonances show up in both transmission and absorption as high-Q states on top of an otherwise undulating background of Fabry-Pérot resonances from the slab; this kind of background would occur even if the slab were uniform. In the case of no absorption, the transmission peaks would go all the way up to 1 and all the way down to 0, but with absorption, they are rounded out somewhat, though their frequencies remain essentially the same; the frequencies are determined by the frequencies of the modes of the corresponding transverse wave vector of the PhC slab. As can be seen

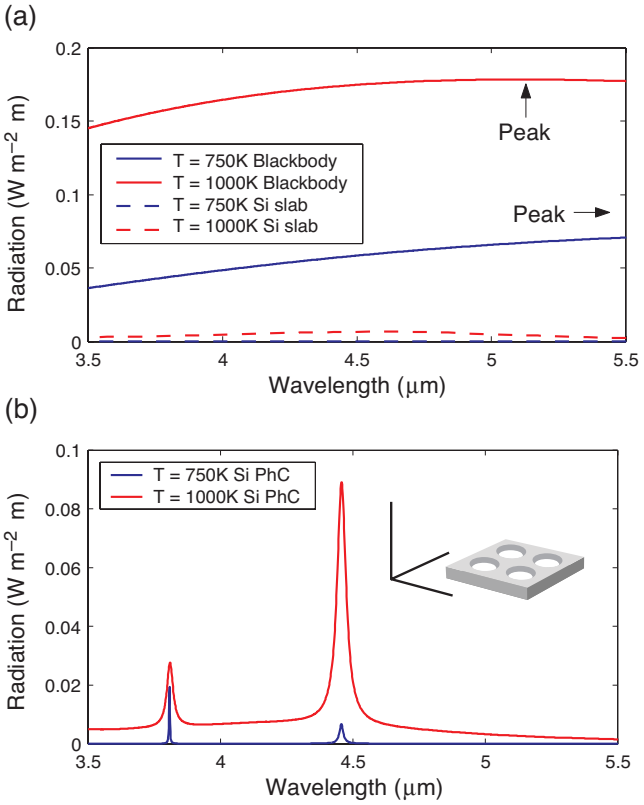

FIG. 1. (Color) Panel (a) shows some generic features associated with thermal radiation of common blackbodies or graybodies into air (the case of a perfect blackbody is denoted by solid lines, while an example of a graybody, a uniform Si slab of thickness 0.75 μm, is denoted by dashed lines); plotted is the (thermal radiation intensity)/$dk_x dk_y d\lambda$ for an exemplary case: k_x=0.838 μm^{-1} and k_y=0. First, blackbodies or graybodies have perfectly incoherent and ultrabroad bandwidth thermal-emission spectra. Next, as the temperature of such a body increases, the emission spectrum shifts to shorter wavelengths. Finally, bodies with lower absorption have weaker thermal emission; for example, a thin silicon slab is nearly transparent for infrared light even at fairly high temperatures, so its thermal-emission is very weak. Panel (b) shows FDTD calculations of the thermal emission spectra of the same Si slab as in panel (a), but this time patterned as a square-lattice 2D-periodic photonic crystal slab of holes with radius r=0.3 μm, and lattice constant a=1.5 μm (structure schematic shown in the inset). Thermal radiation of such a body can display drastically different behavior than the one shown in panel (a). First, a photonic crystal can produce very coherent thermal radiation, as implied by the narrowness of the emission peaks. Next, as one increases the temperature, the peak emission can shift to longer (instead of shorter) wavelengths. Finally, despite the near-transparency of Si, emissivity can be comparable to that of a perfect blackbody for certain frequencies.

from Fig. 2(b), as one increases the angle of incidence (k_x), some resonances increase in frequency while others decrease. Still others remain unchanged (these are flat bands).

Turning closer attention to the absorption spectrum in Fig. 2(a), we observe first of all that the background absorption of the slab is very low, in the region of 2–3 %. However, of more interest are the strong absorption peaks on top of the background, in some cases reaching 50%. This illustrates

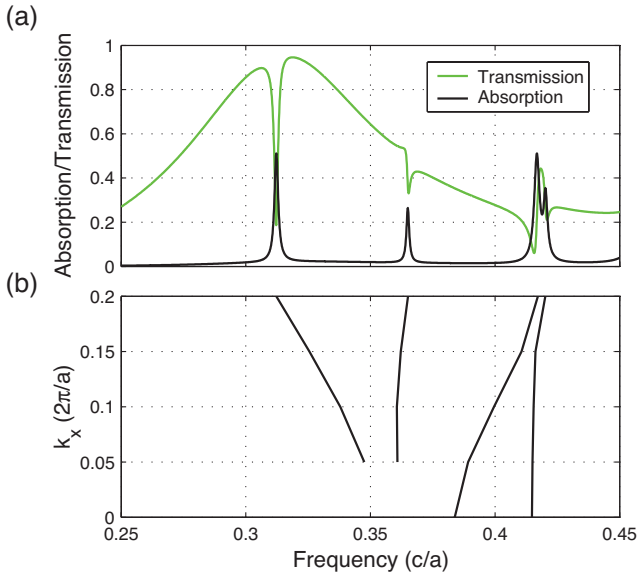

FIG. 2. (Color) FDTD simulations of a photonic crystal slab (PhC) of thickness 0.5a with Re(ϵ)=12 for incident electric field polarized in the y direction. (a) Transmission and absorption spectra for a PhC slab, for k_x=0.2(2π/a), with Im(ϵ)$\approx$0.005 (chosen to maximize absorption for the first peak), displaying four Fano resonance peaks. (b) Band diagram of the photonic crystal slab modes in the case of an infinitesimally small amount of absorption. Note that Fano resonances in panel (a) occur exactly at those frequencies for which there is a guided mode of the PhC that has k_x=0.2(2π/a).

how greatly Fano resonances can enhance absorption over and above that for the slab. Now, Kirchhoff's law states that emissivity and absorptivity are equal, meaning that for Fano resonance frequencies the *emissivity* of the PhC slab can approach that of a perfect blackbody.

To identify the important physical parameters of the system and their relationship to PhC emissivity, we study the behavior of Fano resonances within a framework of coupled-mode theory [20]. By extending the analysis of Ref. [18] to an absorptive case, we determine that the absorption coefficient of the PhC slab is given by

$$|a_{\mathrm{PhC}}|^2 = \frac{2\gamma_{rad}\gamma_{abs}}{(\omega-\omega_0)^2+(\gamma_{rad}+\gamma_{abs})^2}, \qquad (1)$$

where ω_0 is the resonant frequency of the resonator, γ_{rad} is the decay rate of the cavity mode in the case of no absorption, and γ_{abs} is the decay rate due to material absorption. Clearly, absorptivity (and therefore, emissivity) is maximized when $\gamma_{\mathrm{rad}}=\gamma_{abs}$. In terms of quality factors ($Q_{rad}\equiv\omega_0/2\gamma_{rad}$), this means $Q_{rad}=Q_{abs}$, i.e., absorption is maximized when the Q_{rad} of the Fano resonance is exactly matched with the absorptive Q_{abs} of the guided mode. When $Q_{rad}=Q_{abs}$, $|a_{\mathrm{PhC}}|^2_{max}$=50%. Note that according to perturbation theory in small ϵ_i [21], $Q_{abs}=\epsilon_r/(\epsilon_i\xi)$ where $\epsilon_{r,i}$ are the real and imaginary parts of the dielectric function, respectively, and ξ is the fraction of modal energy contained within the dielectric. Note that Eq. (1) and the expression for Q_{abs} provide us with a physical model that can be used for under-

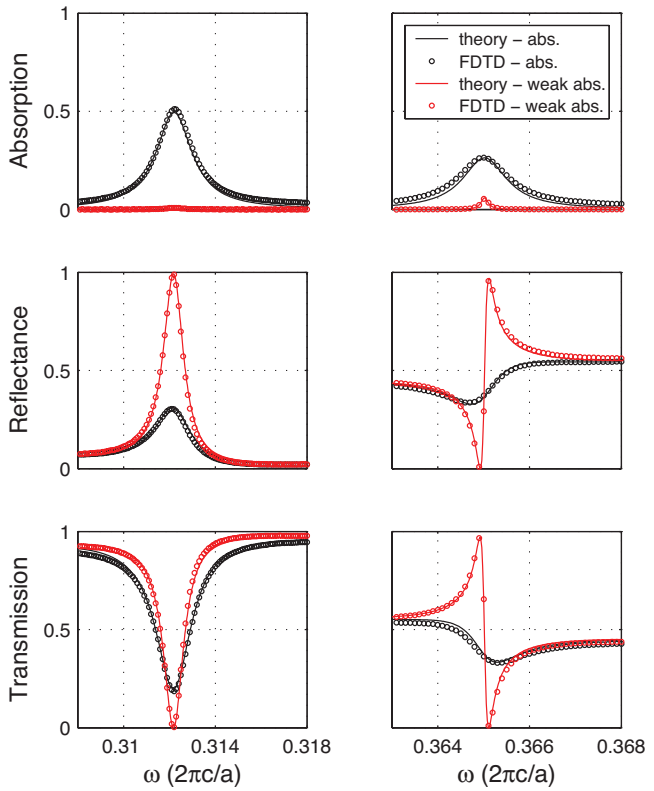

FIG. 3. (Color) Comparison between theory and simulation, for the first two Fano peaks shown in Fig. 2(a). The parameters of the theory (ω_0 and γ_{rad}) were calibrated by fitting the red line (theory with vanishingly small absorption) to the red circles (simulation with vanishingly small absorption). The black line gives the prediction of theory for the absorptive case; the black circles represent the results from simulation with absorption. (The fraction of energy in dielectric (ξ) was 90% for the first peak and 95% for the second, done in a separate FDTD calculation.)

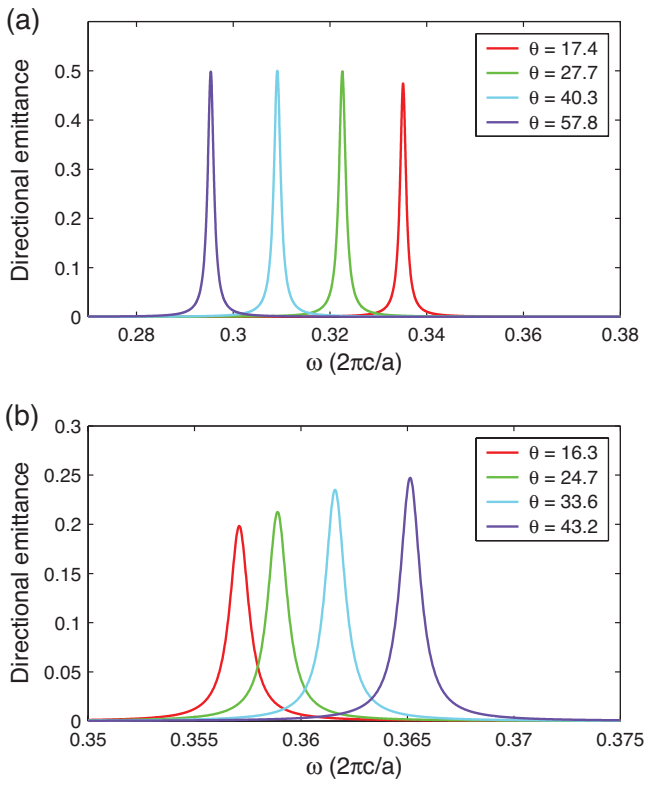

FIG. 4. (Color) Variation of Fano absorption peak frequency as a function of angle of incidence (in degrees); the rotation angle θ is around the y axis, and the electric field is polarized along y. (a) First peak. (b) Second peak. The change in frequency for the second peak is much smaller than that for the first. The angles are different for the top and bottom panels even though the k_x's used are the same because θ is a function of both k_x' and ω.

standing anomalous thermal behavior. In a similar fashion, one obtains

$$|t_{\mathrm{PhC}}|^2 = \left| t_{slab} - \frac{(t_{slab} \pm r_{slab})\gamma_{rad}}{i(\omega - \omega_0) + \gamma_{rad} + \gamma_{abs}} \right|^2,$$

$$|r_{\mathrm{PhC}}|^2 = \left| r_{slab} - \frac{(r_{slab} \pm t_{slab})\gamma_{rad}}{i(\omega - \omega_0) + \gamma_{rad} + \gamma_{abs}} \right|^2,$$

where r_{slab} and t_{slab} are the reflection and transmission coefficients, respectively, of the planar slab without any holes. Note that r_{slab} and t_{slab} are complex functions that incorporate the phase change upon transmission and reflection.

Let us now test this model against numerical simulations in order to validate our theory. Numerical simulations in our work are performed using a finite-difference time-domain (FDTD) algorithm [22] with a resolution of 30 grid points per lattice constant (a). These are exact 3D solutions of Maxwell's equations, including material dispersion and absorption. Reflectance is given by $R(\omega) = [\Phi_1^{vac}(\omega) - \Phi_1^{slab}(\omega)]/\Phi_1^{vac}(\omega)$ where the flux plane closer to the light source is "1," and the flux plane further from the light source is "2." The transmission is given by $T(\omega) = \Phi_2^{slab}(\omega)/\Phi_2^{vac}(\omega)$ and the absorption is simply $A(\omega) = 1 - R(\omega) - T(\omega)$. This way, we obtain reflectance, transmission, and absorption spectra for PhC slabs. We repeat these calculations for incident light with different transverse wave vectors (k_x). From these spectra, the resonant frequencies and widths (i.e., lifetimes) of Fano resonances can be extracted. We incorporate absorption into our simulations by means of the Drude model, according to the following equation: $\epsilon(\omega) = \epsilon_\infty + \sigma/(\omega_0^2 - \omega^2 - i\gamma\omega)$ where ϵ_∞, γ, ω_0, and σ are input parameters. These are chosen so as to produce the desired absorption [$\mathrm{Im}(\epsilon)$] at the frequencies we are interested in. We show the results in Fig. 3. The two different Fano peaks shown in Fig. 3 display qualitatively fairly different behavior, as has been previously elaborated in Ref. [18]. First, we plot transmission, reflectance and absorption in the nearly lossless case ($\gamma_{abs} < 3 \times 10^{-6}$) for the first two Fano peaks shown in Fig. 2(b) (red circles in Fig. 3); then ω_0 and γ_{rad} were extracted from these results, and analytical predictions (red lines) were obtained. Note that γ_{rad} was also calculated directly by solving Maxwell's equations numerically and performing a harmonic inversion on the time-series data. Indeed, the fitted value and the directly calculated value agree very well, to within a couple of percent. We then plot the numerical results with absorption (black circles), and the predictions of the model (black lines).

We see very good agreement between theory and simulation. The imaginary part (ϵ_i) of the material in the absorptive case was chosen such that there is near-perfect matching between the Q_{rad} of the first resonance ($\approx$370) and the absorptive Q of the material: $Q_{abs}=Q_{rad}$, which causes the absorption to be maximized. We see this clearly in the first panel, where the absorption coefficient (black line and circles) hits 50%. The same is not true of the second peak, because the Q_{rad} of that peak ($\approx$2000) is much higher than $Q_{abs}=370$, so there is poor Q matching and thus weaker absorption. Nonetheless, the fit between theory and simulation is excellent.

Confident that our analytical model has been validated by numerical studies, we proceed to use this model to modify the thermal behavior of PhC systems. We have shown that low emissivities of uniform slabs can be greatly enhanced by means of Fano resonances. The frequencies of these emission peaks are determined by the frequencies of Fano resonances, while the heights of these peaks are determined by how well Q_{abs} matches with Q_{rad}. The exact positions of Fano frequencies can be controlled by the geometry of the PhC (slab thickness, a, ϵ_r, and to some extent hole sizes), which determines guided modes. Q_{rad} is determined by the strength of the coupling of guided modes to radiation (controlled mostly by the size of the holes). Q_{abs} is determined by ϵ_i, and the overlap of the guided modes with absorptive regions of the structure. Given that one has so many parameters to control, and that their influence is largely decoupled, one can tail or properties of thermal radiation almost at will.

In fact, most of the relevant parameters can even be controlled dynamically. For example, changes in geometry can be implemented mechanically at ms-μs time scales (e.g., MEMS). Similarly, changes of ϵ_r, ϵ_i can be implemented via change of temperature, or using electro-optical effects, or carrier injection (this can change ϵ_i by orders of magnitude); some of these effects can be operated at subnanosecond time scales.

As an illustrative example, we present the case where ϵ_i varies with temperature. In the case of silicon, the imaginary part of the dielectric function is strongly temperature-dependent, and increasing the temperature from, say, 750 to 1000 K increases the imaginary part in the ir regime from 10^{-3} to 10^{-2}, i.e., by a factor of 10 [23]. (The real part changes by 3% or so. We use the following expressions for the temperature-dependent refractive index for silicon: $n_{\mathrm{Si}}=16.044(1000\lambda)^{-0.194}$ and $k_{\mathrm{Si}}=(\alpha/4\pi)\lambda\times10^{-4}$, where $\alpha=4.15\times10^{-5}\lambda^{1.51}T^{2.95}e^{-7000/T}$, with λ specified in μm and α in cm^{-1}.) At 750 K, $Q_{abs}\sim1000$ and the higher-frequency Fano peak [at around 4.5 μm in Fig. 1(b)] is more closely matched with Q_{abs} than the lower-frequency peak, resulting in a higher emissivity. At 1000 K, $Q_{abs}\sim100$ and the lower-frequency Fano peak (at around 3.8 μm) is better matched, resulting in emissivity close to 50%. In other words, as we heat up this 2D silicon PhC slab, we see peak emission move from short to long wavelength. This is precisely the opposite of what is expected from a typical graybody, where the wavelength of strongest emission decreases with temperature. Note that the position of each emissivity peak is fairly independent of the temperature, which is also markedly different than in ordinary graybodies. This anomalous emissivity behavior occurs as a result of a peculiar interplay between $Q_{abs}(T)$ and the Q_{rad} of the Fano resonances.

Of further interest is the fact that thermal-emission properties can have rich dependence on the angle of observation. Figure 4 shows the variation in the frequency of the emissivity peak with respect to change in angle. In the top panel, plotted for the low-frequency Fano resonance from Fig. 2(a), we see that as we move away from normal incidence, the frequency of the peak decreases. This can be understood from the band diagram for Fano resonances in Fig. 2(b), which shows decreasing ω with increasing k_x (a proxy for angle of incidence) for the first band. In the bottom panel, we plot the same variation for the second peak. This agrees with the band diagram again in Fig. 2(b), which shows a relatively flat second band.

This work was supported in part by the Croucher Foundation (Hong Kong) and the MRSEC program of the NSF under Grant No. DMR-0213282.

[1] S. Y. Lin *et al.*, Nature (London) **394**, 251 (1998).
[2] S.-Y. Lin *et al.*, Phys. Rev. B **62**, R2243 (2000).
[3] H. Sai *et al.*, J. Opt. Soc. Am. A **18**, 1471 (2001).
[4] J. G. Fleming *et al.*, Nature (London) **417**, 52 (2002).
[5] S. Y. Lin *et al.*, Appl. Phys. Lett. **83**, 380 (2003).
[6] S.-Y. Lin *et al.*, Appl. Phys. Lett. **84**, 1999 (2004).
[7] H. Sai *et al.*, Thermophotovoltaic generation with microstructured tungsten selective emitters, in *Proceedings of the Sixth NREL Conference on Thermophotovoltaic Generation of Electricity* (AIP, New York,2004), pp. 206–214.
[8] C. Luo *et al.*, Phys. Rev. Lett. **93**, 213905 (2004).
[9] M. Florescu *et al.*, Phys. Rev. A **72**, 033821 (2005).
[10] C. M. Cornelius and J. P. Dowling, Phys. Rev. A **59**, 4736 (1999).
[11] A. Narayanaswamy and G. Chen, Phys. Rev. B **70**, 125101 (2004).
[12] J.-J. Greffet *et al.*, Nature **416**, 61 (2002).
[13] B. J. Lee *et al.*, Appl. Phys. Lett. **87**, 071904 (2005).
[14] I. Celanovic *et al.*, Phys. Rev. B **72**, 075127 (2005).
[15] A. Yariv, IEEE Photonics Technol. Lett. **14**, 483 (2002).
[16] M. U. Pralle *et al.*, Appl. Phys. Lett. **81**, 4685 (2002).
[17] S. Enoch *et al.*, Appl. Phys. Lett. **86**, 261101 (2005).
[18] S. Fan and J. D. Joannopoulos, Phys. Rev. B **65**, 235112 (2002).
[19] M. Laroche *et al.*, Phys. Rev. Lett. **96**, 123903 (2006).
[20] H. A. Haus, *Waves and Fields in Optoelectronics* (Prentice-Hall, Englewood Cliffs, NJ, 1984).
[21] M. Soljacic *et al.*, Phys. Rev. E **71**, 026602 (2005).
[22] A. Taflove and S. C. Hagness, *Computational Electrodynamics: The Finite-Difference Time-Domain Method* (Artech House, Norwood, MA, 2000).
[23] D. Chub *et al.*, Semiconductor Silicon as Selective Emitter, in *TPV Generation of Electricity 5th Conference*, AIP Conf. Proc. No. 653 (AIP, New York, 2003), 174–200.